

## Hardness of nanocrystalline diamonds

John S. Tse,<sup>1,\*</sup> Dennis D. Klug,<sup>2,\*</sup> and Faming Gao<sup>2</sup>

<sup>1</sup>*Department of Physics and Engineering Physics, University of Saskatchewan, Saskatoon, S7N 5E2, Canada*

<sup>2</sup>*Steacie Institute for Molecular Sciences, National Research Council of Canada, Ottawa, K1A 0R6, Canada*

(Received 6 December 2005; published 24 April 2006)

The predicted static and dynamical properties of a recently reported 6H polymorph of diamond based on first-principles electronic structure calculations are reported. Although 6H diamond is less stable than the cubic 3C phase, it is found to exhibit similar mechanical properties. The hardness predicted using a semiempirical theory developed recently is found to be comparable to cubic diamond. This theory, extended to nanocrystals by including quantum confinement effects, elucidates the superhardness recently reported in nano 3C and 6H diamond crystallites that were shown to exceed that of the bulk diamond. The method provides a theoretical tool for the characterization and design of other nanohardened materials.

DOI: [10.1103/PhysRevB.73.140102](https://doi.org/10.1103/PhysRevB.73.140102)

PACS number(s): 62.20.Qp, 71.15.Mb

The cubic ( $Fd\bar{3}m$ ) 3C phase is the most studied form of diamond. The exceptional physical properties of the 3C phase make it, not only as an outstanding gem, but also as a technologically important material in a wide variety of industrial applications. In the Mohs' scale of hardness, 3C diamond is considered to be the hardest crystal. Over the last two decades, many theoretical and experimental investigations have been devoted to the search for novel materials, with hardness exceeding that of the 3C diamond.<sup>1-5</sup> Besides the conventional cubic structure, diamond is also known to exist in a number of forms. One of the strategies in the search for superhard materials has been on the fabrication and characterization of these forms of diamond. Recently, several exciting experimental results have been reported.<sup>6,7</sup> In particular, a mixture of hexagonal 2H, 4H, 6H, 8H, 10H, and rhombohedral 15R diamonds have been found in thin films grown by chemical vapor deposition (CVD).<sup>8,9</sup> Since the hardness of these thin films is determined by the combined properties of the constituents, studies on the origin of hardness of the polymorphs are highly relevant. Moreover, ultrahard polycrystalline pure cubic diamond has been synthesized from graphite, and the Knoop hardness was found to be 110–140 GPa, which exceeds the hardness of bulk diamond of 60–120 GPa.<sup>6</sup> Diamond nanorods with 5–20 nm diameters have also recently been prepared from C<sub>60</sub> that have higher bulk moduli than that of bulk diamond and appear to be harder than bulk diamond.<sup>10</sup> More recently, a powder sample of a nanophase 6H polymorph has been prepared by high temperature-high pressure synthesis from C<sub>60</sub>,<sup>11,12</sup> and its hardness was claimed to surpass that of the 3C diamond.<sup>12</sup> At first sight, it is highly unusual that the hexagonal phase can be harder than the cubic phase. In this Letter, we offer a theoretical basis to rationalize the experimental observation. The understanding and characterization of this novel property have been hindered by the practical problems to obtain pure crystalline samples. To this end, a first-principles technique is employed to predict the electronic, static, elastic, and dynamical properties. The results of the calculations in combination with the development of a semiempirical method for the prediction of the hardness of nanocrystallites provide a detailed understanding on the stability and physical properties of bulk and nanophase 6H diamond.

6H diamond has a  $P6_3/mmc$  space group symmetry. The

hexagonal unit cell is shown in Fig. 1. Calculations of the optimized geometries, energetics, elastic moduli, and phonon band structure were carried out in the framework of density functional theory (DFT) with the Vienna *Ab-initio* Simulation Package (VASP).<sup>13,14</sup> The interactions between the ions and the electrons are described by Vanderbilt ultrasoft pseudopotential.<sup>15</sup>

Electron-electron interactions are treated within the generalized gradient approximation (GGA) by the Perdew-Burke-Ernzerhof (PBE) exchange correlation functional.<sup>16</sup> The calculations were performed by using an energy cutoff of 500 eV with the plane wave basis set. Brillouin zone (BZ) integration was performed using the special  $k$ -point Monkhorst-Pack sampling scheme. In the geometry optimization, all the atomic coordinates and unit cell parameters were relaxed with a conjugate gradient (CG) algorithm subject to a force tolerance of  $<0.001$  eV/Å. The elastic moduli were evaluated using the stress-strain relationship<sup>17</sup> and the phonon bandstructure using the supercell method.<sup>18</sup>

The structures, energetics, and properties obtained from first-principles calculation for 6H diamond is compared with the 3C phase in Table I. The agreement between predicted properties with available experimental data is excellent. The total energy of the 6H phase is less than 3C by only

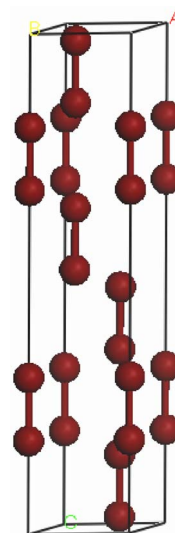


FIG. 1. (Color online) The crystal structure of 6H diamond.

TABLE I. Theoretical values of equilibrium structural parameters, total energies  $E_0$  (eV/atom), elastic constants  $C_{ij}$  (GPa), shear modulus  $G$  (GPa), bulk modulus  $B_0$  (GPa), and its pressure derivative  $B'_0$ . For comparison, other experimental and calculated results are also given in parentheses.

Property	6H-diamond	3C-diamond	6H-SiC	3C-SiC
Crystal system	Hexagonal	Cubic	Hexagonal	Cubic
Space group	$P6_3/mmc$	$Fd\bar{3}m$	$P6_3/mmc$	$Fd\bar{3}m$
Atoms/unit cell	12	8	12	8
Cell constants (Å)	$a=2.522$ (2.490, <sup>a</sup> 2.510 <sup>b</sup> ) $c=12.4462$ (12.282, <sup>a</sup> 12.301 <sup>b</sup> )	$a=2.522$ (2.522 <sup>c</sup> )	$a=3.093$ $c=15.1453$	$a=3.037$
$E_0$ (eV/atom)	-9.0911	-9.0971	-7.7021	-7.5480
$C_{11}$ (GPa)	1158	1059		
$C_{12}$	95	134		
$C_{13}$	45			
$C_{33}$	1210			
$C_{44}$	480	562		
$G$ (GPa)	521	525		
$B_0$ (GPa)	433 (471 <sup>a</sup> )	443(471, <sup>a</sup> 442 <sup>c</sup> )	215	212
$B'_0$	3.6 (3.7 <sup>a</sup> )	3.8 (3.7 <sup>a</sup> )	3.9	3.9
$E_g$ (eV) <sup>d</sup>	6.08	5.67 (5.48) <sup>e</sup>		

<sup>a</sup>Calculated value from Ref. 19.

<sup>b</sup>Experimental value from Ref. 11.

<sup>c</sup>Experimental value from Ref. 19.

<sup>d</sup>Indirect bandgap calculated with B3LYP functional (see the text).

<sup>e</sup>Experimental value at 0 K.

0.14 kcal/atom. Therefore, 6H is metastable with respect to 3C diamond, so it is not surprising that the growth of 6H polymorph of diamond often require nonequilibrium conditions such as rapid implosion in meteorites, manmade explosions, and at high temperature-high pressure. The predicted bulk (433 GPa) and shear moduli ( $G$ , 521 GPa) of the 6H phase is somewhat smaller than the corresponding values (443 and 525 GPa, respectively) for 3C diamond. This observation is consistent with the calculated shear elastic constant  $C_{44}$  of 480 GPa for 6H, which is also less than that of 3C of 592 GPa. 6H diamond is found to be an indirect bandgap semiconductor. The estimated bandgap energy (from a hybrid B3LYP functional) that has been shown to give an improved bandgap energy for semiconductors<sup>19</sup> of 6.08 eV is higher than that of 3C diamond of 5.67 eV (5.48 eV experimental value at 0 K). The band structures are similar to those reported for carbon polymorphs earlier<sup>20</sup> using a DFT-LDA method, although the bandgaps differ, as expected for the different exchange-correlation functional used. The calculated phonon band structure and vibrational density of state is shown in Fig. 2. At the zone center ( $\Gamma$ ) vibrational bands are “clustered” at 286, 470–540, 860, 1050, and 1200–1300  $\text{cm}^{-1}$ . No vibrational spectrum for pure 6H diamond is available in the literature. The Raman spectrum of carbon materials obtained from  $C_{60}$  treated at 2200 K at 20 GPa<sup>12</sup> shows a broad distribution of vibrational modes with band maxima located at 500, 1100, and 1420  $\text{cm}^{-1}$ . Two and three phonon features were observed at *ca.* 1100, 2000, 2500  $\text{cm}^{-1}$  in the IR spectrum.<sup>12</sup> Additional phonon calcula-

tions up to 250 GPa show that the 6H diamond is stable within this pressure range.

Microhardness is an intrinsic property of a material and is often used to evaluate the mechanical properties of bulk solids and thin films. The ability to predict hardness is of great importance because it will be very helpful to understand the hardening mechanism and for the exploration of new superhard materials. Recently a semiempirical model has been proposed<sup>21,22</sup> to give a quantitative estimate of hardness. This model defines hardness as the sum of the resistance of each bond per unit area to indentation. According to this approach, the hardness ( $H_v$ ) of a covalent crystal is given as

$$H_v = \left[ \prod (H_v^\mu)^{n^\mu} \right]^{1/\sum n^\mu}, \quad (1)$$

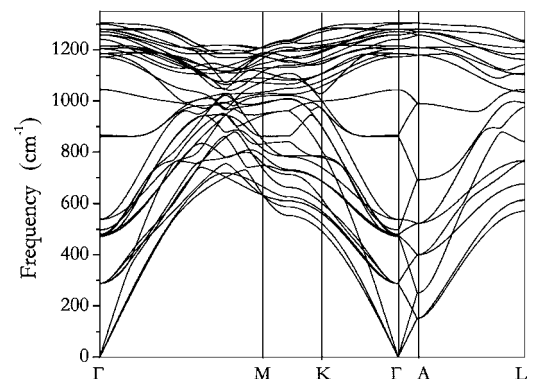


FIG. 2. Theoretical phonon band structure of 6H diamond at ambient pressure.

TABLE II. Hardness and parameters related to the hardness calculations of the 6H diamond, 3C diamond, 6H-SiC, and 3C-SiC, where  $H_{v \text{ calc.}}$  and  $H_{v \text{ exp.}}$  are calculated and experimental microhardness, respectively.

Phase	Bond length	$N_e^\mu$	$f_i^\mu$	$H_v^\mu$	$H_{v \text{ cal}}$ (GPa)	$H_{v \text{ exp}}$ (GPa)	$H_{v \text{ cal nano}}$ (GPa)
6H diamond	1.547 ( $\times 2$ )	0.702		93	93		96 (5 nm)
	1.570 ( $\times 2$ )	0.672		87		94 (12 nm)	
	1.545 ( $\times 4$ )	0.704		93		108 (1.245 nm)	
	1.546 ( $\times 6$ )	0.703		93			
3C diamond	1.545	0.705			94	96 <sup>a</sup>	97 (5 nm)
							95 (12 nm)
							112 (1.0 nm)
6H SiC	1.890 (av)	0.386	0.190		30	21–31 <sup>b</sup>	
3C SiC	1.860	0.404	0.177		33	34 <sup>a</sup>	

<sup>a</sup>Experimental value from Ref. 20.

<sup>b</sup>Experimental value from Ref. 32.

$$H_v^\mu (\text{GPa}) = 8.82(N_e^\mu)^{2/3} E_h^\mu e^{-1.191f_i^\mu} \\ = 350(N_e^\mu)^{2/3} e^{-1.191f_i^\mu} / (d^\mu)^{2.5}, \quad (2)$$

where  $n_\mu$  is the number of bond of type  $\mu$  composing the crystal and  $d^\mu$  is the bond length in angstroms.  $N_e^\mu$  is the numbers of valence electrons of the type  $\mu$  bond per unit volume.  $f_i^\mu$  is the ionicity, and  $E_h^\mu$  is the “pseudo”-energy of the homopolar gap.

The hardness of 6H diamond can be predicted using Eq. (2). The results and relevant parameters are reported in Table II. For comparison and to validate the model, calculated results for 3C diamond, the 6H and 3C-SiC analogs are also included. Agreement with experiment is exceedingly good. The predicted hardness for 3C diamond in the Vickers scale of 94 GPa is very close to the measured hardness of 96 GPa.

The predicted hardness of the 6H phase of 93 GPa is only slightly lower than bulk diamond. A smaller hardness in 6H diamond is not unexpected since the calculated shear moduli (both  $G$  and  $C_{44}$ , *vide supra*), which has been shown to be an indicator of hardness, are also smaller than 3C diamond. A smaller hardness of the hexagonal as compared to the cubic structure is also observed in the closely related SiC polymorphs. Once again, the semiempirical model correctly predicts the experimental trend. The calculated hardness for 3C and 6H SiC is 37 and 30 GPa, respectively. These values compare very well with the observed values of 34 GPa and 21–31 GPa. The results presented here show that the semiempirical model is reliable and capable to provide quantitative hardness values for comparison with experiment.

In recent experiments, nanocrystalline samples of cubic 3C diamond and the 6H polymorph with crystallite sizes of 5–12 nm have been synthesized from high temperature and high pressure compression of graphite<sup>6</sup> and from  $C_{60}$ <sup>12</sup> with multianvils. Although the claims of superhardness must be viewed with caution,<sup>23</sup> indentation experiments on nanopolycrystalline (10–30 nm) 3C diamond show Knoop hardness of 110–145 GPa.<sup>24</sup> This value is to be compared with bulk diamond of 60–120 GPa. It was also reported that microcrystallites 6H diamond could scratch the surface of bulk diamond.<sup>12</sup> These are remarkable and important observations. A

Vickers-type indenter is known not to make any scratches or indentations on the surface of nanodiamonds at loads up to 500 g.<sup>12</sup> According to the Mohs’ scale of hardness, the appearance of scratch marks indicates that nanocrystalline 6H diamonds may be harder than bulk 3C diamond. Apparently, nanosize-induced effects can result in a significant increase of hardness of nano 3C and 6H diamonds.

This novel observation can be explained by combining the theory of hardness<sup>21</sup> with quantum confinement effects. For a pure covalent crystal, such as 3C diamond and 6H diamond, the hardness can be expressed as  $H$  (GPa) =  $AN_a E_g$ , where  $N_a$  is the number of covalent bond per unit area, where  $A$  is a proportionality constant, and  $E_g$  is the “effective” bandgap. This relationship implies that the hardness of a crystal is proportional to the bandgap. On the other hand, it is well known that the quantum-size effect plays an important role on the bandgap of semiconductor nanocrystals. In nanocrystals, the conduction/valence band edges generally to shift to higher energy relative to the bulk material when the crystalline size is decreased. According to the Kubo theory,<sup>25</sup> the bandgap ( $E_{g \text{ nano}}$ ) of a nanocrystal should increase inversely with the volume  $V$ ,

$$E_{g \text{ nano}} = E_{g \text{ bulk}} + \delta, \quad (3)$$

where  $E_{g \text{ bulk}}$  is the “effective” bandgap energy of the bulk material.  $\delta$  is the energy shift, and is given by

$$\delta = \frac{2\hbar^2 \pi^2}{mV(3\pi^2 N_e)^{1/3}}, \quad (4)$$

where  $m$  is the atomic mass and  $N_e$  is the electron density of the material.

The theory of hardness is based on the average energy band model.<sup>21,22</sup> When Eq. (4) is extended to include quantum confinement effects for nanocrystals, the energy shift of a nanocrystallite  $\delta_p$  can be written as

$$\delta_p = K \frac{2\hbar^2 \pi^2}{mV(3\pi^2 N_e)^{1/3}} = \left( K \frac{2\hbar^2 \pi^2}{mV(3\pi^2)^{1/3}} \right) N_e^{-1/3} = f(D) N_e^{-1/3}, \quad (5)$$

where the parameter  $K$  may also be a function of the particle diameter. We can approximate the term in the brackets of Eq. (5) as a function of the cluster diameter  $D$ ,  $f(D)$ . Equating

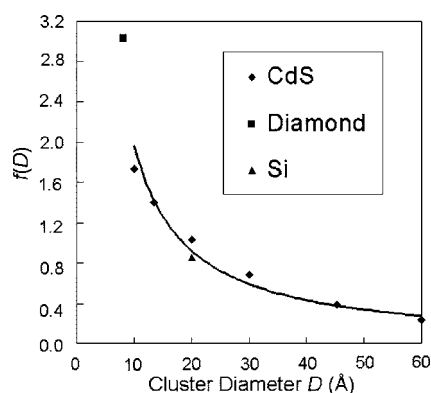


FIG. 3.  $f(D)$  as defined in Eq. (5) as a function of cluster diameter  $D$ .

the band shift ratio to experimental shift ratio:  $\delta_p/E_{gp} = \delta/E_g$ , and using CdS as a calibrant, the bracketed term in Eq. (5) can be evaluated. We found that an empirical formula with  $\delta_p$  inversely proportional to the cluster diameter  $D$  gave a good fit to the experimental data of nanocrystalline CdS (see Fig. 3, later),<sup>26</sup>

$$\delta_p = \frac{24.0}{DN_e^{1/3}} \text{ (eV)}. \quad (6)$$

To validate this relationship, we estimate the bandgaps of nanodiamond and silicon<sup>27–29</sup> and compare with the corresponding experimental data in Fig. 3. The agreement is exceedingly good. Encouraged by this result, an expression for the hardness of a nanocrystal can be obtained by substituting Eq. (6) into Eq. (3),

$$H \text{ (GPa)} = AN_a(E_{g \text{ bulk}} + \delta_p) = AN_a(E_{g \text{ bulk}} + 24.0/DN_e^{1/3}). \quad (7)$$

This formula is used to compute the hardness of the nano 6H and nano 3C diamond and the results are given in Table II. These results are remarkable and highly significant. It is shown that the hardness of the nano 6H and nano 3C diamond with crystallite sizes of 5–12 nm can in fact be larger

than that of bulk diamond. The theoretical prediction is in good accord with the observed superhardness in nanocrystalline 3C<sup>6</sup> and 6H diamonds.<sup>12</sup> Since the predicted hardness of bulk 6H diamond is very close to that of an ordinary cubic diamond, the addition of the quantum confinement effect raises the hardness of the nano 6H diamond, making it even harder than the bulk 3C diamond. This conclusion is also consistent with a recent report<sup>6</sup> that the nanocrystalline 3C diamond has a hardness significantly higher than the bulk single crystal. Remarkably, the predicted Vicker's hardness for a 10 nm 3C diamond of  $\sim 100$  GPa is indeed very close to the estimated value of diamond nanorods with a diameter of 5–20 nm.<sup>10</sup> If one assumes that the minimum size of a nanocrystallite size should be in the order of a nanometer,<sup>30</sup> one can estimate the limit of nanohardening of the nano 6H diamond and nano 3C diamond as 108 and 112 GPa, respectively (see Table II). A Knoop hardness as high as 145 GPa for a nanocrystalline 3C diamond has also been reported,<sup>31</sup> but hardness measurements on materials with values near that of diamond are subject to a good deal of uncertainty.<sup>23</sup> The predicted percentage enhancement of hardness for nano-sized material is consistent with that of Ref. 31.

In conclusion, the structure, energetic, mechanical, elastic, and dynamical properties of the 6H diamond have been predicted from first-principles calculations. A semiempirical method of hardness has been applied to predict the hardness of the bulk 6H diamond. The results show that the bulk modulus and hardness of the bulk 6H diamond is only slightly lower than that of a cubic diamond. This semiempirical model is further extended to nanocrystallites by including the effect of quantum confinement to the bandgap energy. This modified model predicts that the nanocrystal should have a larger hardness than the corresponding bulk material. The theoretical results help to elucidate the recent observation that nano 6H and 3C diamond possess a superhardness exceeding that of bulk cubic diamond. The successful application of this model should help the continuing search for novel superhard nanomaterials for industrial applications.

\*Author to whom correspondence should be addressed. Electronic address: John.Tse@usask.ca; Dennis.Klug@nrc.ca

<sup>1</sup>R. Riedel, *Handbook of Ceramic Hard Materials* (Wiley-VCH, Weinheim, 2000).

<sup>2</sup>A. Y. Liu and M. L. Cohen, *Science* **245**, 841 (1989).

<sup>3</sup>D. M. Teter and R. J. Hemley, *Science* **271**, 53 (1996).

<sup>4</sup>J. Haines *et al.*, *Annu. Rev. Mater. Res.* **31**, 1–13 (2001).

<sup>5</sup>V. L. Solozhenko *et al.*, *Appl. Phys. Lett.* **78**, 1385 (2001).

<sup>6</sup>T. Irifune *et al.*, *Nature* **421**, 599 (2003).

<sup>7</sup>Z. Wang *et al.*, *Proc. Natl. Acad. Sci. U.S.A.* **101**, 13699 (2004).

<sup>8</sup>M. Frenklach *et al.*, *J. Appl. Phys.* **66**, 395 (1989).

<sup>9</sup>R. Kapil *et al.*, *Appl. Phys. Lett.* **68**, 2520 (1996).

<sup>10</sup>N. Dubrovinskaia *et al.*, *Appl. Phys. Lett.* **87**, 083106 (2005).

<sup>11</sup>P. D. Ownby, *Technical Proceedings of the 2004 NSTI Nanotechnology Conference and Trade Show*, 2004, Vol. 3, p. 210.

<sup>12</sup>N. Dubrovinskaia *et al.*, *Diamond Relat. Mater.* **14**, 16 (2005).

<sup>13</sup>G. Kresse and J. Furthmuller, *Comput. Mater. Sci.* **6**, 15 (1996).

<sup>14</sup>G. Kresse and J. Furthmuller, *Phys. Rev. B* **54**, 11169 (1996).

<sup>15</sup>D. Vanderbilt, *Phys. Rev. B* **41**, R7892 (1990).

<sup>16</sup>J. P. Perdew *et al.*, *Phys. Rev. Lett.* **77**, 3865 (1996).

<sup>17</sup>Y. Le Page *et al.*, *J. Appl. Crystallogr.* **38**, 697 (2005).

<sup>18</sup>Z. Li and J. S. Tse, *Phys. Rev. B* **61**, 14531 (2000); K. Parlinski *et al.*, *Phys. Rev. Lett.* **78**, 4063 (1997).

<sup>19</sup>J. Muscat *et al.*, *Chem. Phys. Lett.* **342**, 397 (2001).

<sup>20</sup>C. Raffy *et al.*, *Phys. Rev. B* **66**, 075201 (2002).

<sup>21</sup>F. M. Gao *et al.*, *Phys. Rev. Lett.* **91**, 015502 (2003).

<sup>22</sup>F. M. Gao, *Phys. Rev. B* **69**, 094113 (2004).

<sup>23</sup>V. Brazhkin *et al.*, *Nat. Mater.* **3**, 576 (2004).

<sup>24</sup>H. Sumiya *et al.*, *Diamond Relat. Mater.* **13**, 1771 (2004).

<sup>25</sup>W. P. Harlperin, *Rev. Mod. Phys.* **58**, 533 (1986).

<sup>26</sup>Y. Wang and N. Herron, *Phys. Rev. B* **42**, 7253 (1990).

<sup>27</sup>J. Y. Raty *et al.*, *Phys. Rev. Lett.* **90**, 037401 (2003).

<sup>28</sup>Y. K. Chang *et al.*, *Phys. Rev. Lett.* **82**, 5377 (1999).

<sup>29</sup>J. P. Wilcoxon *et al.*, *Phys. Rev. B* **60**, 2704 (1999).

<sup>30</sup>M. V. Rama Krishna *et al.*, *J. Chem. Phys.* **95**, 8309 (1991).

<sup>31</sup>H. Sumiya and T. Irifune, *SEI Technical Review* **59**, 57 (2005).

<sup>32</sup>K. Nihara, *J. Less-Common Met.* **65**, 156 (1979).